Inhibition effect of SiO$_x$ formation and modulation of charge state at SrO/Si(100) interface synthesized by pulsed laser deposition

Yasushi Hotta and Shin-ichi Satoh

University of Hyogo
2167 Shosha, Himeji, Hyogo 671-2280, Japan
Phone: +81-79-267-4976 E-mail: hotta@eng.u-hyogo.ac.jp

1. Introduction

Growth of metal oxide films on Si substrate has been intensively studied from the point of view of incorporation of novel properties into existing Si-base electronics. [1] Metal oxide materials exhibit a wide variety of properties such as high dielectric constant (high-k), [2] ferroelectricity, [3] colossal magnetoresistance, [4] and high-T_C superconducting, [5] and the materials have potential abilities to overcome limitations of the development of the Si-base electronic devices. For example, high-k materials will provide more thinner effective oxide thickness (EOT) of metal-oxide-semiconductor field-effect transistor (MOSFET), [2] and ferroelectrics will be utilized for novel types of nonvolatile memory devices. [3] Though, there are still some technological challenges in the growth of high-quality oxide films on Si substrates. Most critical issue is formation of an interfacial SiO$_x$ layer, which induces degradation of the above devices.

To avoid the SiO$_x$ formation, a buffer layer of metal Sr or SrO is used between the oxide nad the Si substrate. [6, 7] Sr is oxidized more than Si in case of the Sr-Si-O ternary systems, resulting that the SiO$_x$ growth is inhibited. The Sr and SrO buffer layers are fabricated by direct deposition of metal Sr or SrO layer on a 2x1 reconstructed Si surface. Previously, molecular beam epitaxy has been used for the buffer layer growth. [6, 7] On the other hand, we have studied the growth by pulsed layer deposition (PLD) in order to generate another choice for the growth technique. PLD is suitable technique to grow complex metal oxide films, and if it is available for the buffer layer growth, the buffer layer and oxide layers above the buffer layer in one sample can be grown in-situ process using only PLD.

In this study, we present a systematic investigation of the effect to inhibit SiO$_x$ formations for SrO buffer layers synthesized by PLD on Si substrate and an interesting data to imply modulation of the interfacial charge state. X-ray photoemission spectroscopy (XPS) was used to investigate the chemical state of SrO layer and the interface of SrO/Si.

2. Experimental

SrO layers were fabricated on p-type Si(100) substrates (CZ, ρ= 1-10 Ωcm) by pulsed laser deposition using SrO single crystal target. Si(100) wafers were cut into 0.8×0.8 cm^2 pieces and cleaned using a conventional RCA method. [8] Following, the Si(100) piece was immersed in a 10% HF solution for 1 min to remove native oxide layers at the surface. After these treatments, the Si piece is immediately mounted on a sample holder and installed into an ultrahigh vacuum chamber. The SrO layers were grown at substrate temperature of RT and 600℃ in background pressure of < 1×10^{-6} Pa using reflection high-energy electron diffraction (RHEED) to monitor the growth process. KrF excimer laser with a 248 wavelength was used at a repetition rate of 1 Hz. Growth rate of the SrO layers was estimated from RHEED oscillation data for layer-by-layer growth of a SrO layer on SrTiO$_3$ (STO) substrate. Thickness of the SrO layers was kept at ~1.5 nm. After the growth, post-annealing treatment was done in an tube furnace with oxygen flow. Core level spectra of Si $2p$, O $1s$, and Sr $3d$ were measured by XPS in order to evaluate the chemical state of the SrO layers and the SrO/Si interfaces.

3. Result and discussion

We measured XPS spectra of as-deposition and post-annealed samples in order to investigate chemical state of the SrO/Si(100) interface. Upper and lower curve in Fig 1 (a) show core level spectra of Si $2p$ of the SrO/Si(100) and a bare Si(100) as a reference. All the samples were annealed at 600℃ for 120 min. In both curves, the 3/2 and 1/2 spin-orbit doublet components attributable to the Si substrate were observed around 98.2 eV, while the broad peaks identified with overlayer Si atoms were detected at higher-binding-energy regions ranging from 99 to 103 eV. The binding-energy values for both spectra were normalized by the Si $2p$ bulk peak. The main components of the overlayer peaks in their curve are clearly located at the different energy position of 102 eV and 103 eV, and these energy positions correspond to silicate formation for the SrO/Si specimen and SiO$_2$ formation for the reference Si, respectively. [9, 10] The silicate formation is also identified in the O $1s$ core level spectrum of the SrO/Si specimen shown in Fig. 1 (b). Deconvolution of the peak specimen indicates existence of three kinds of components arising from Sr-O, Si-O-Sr, and mono-oxide coordination. [11, 12] As Si-O-Sr is main components, it is considered that a Sr-silicate interfacial layer was formed at the SrO/Si interface by the post-annealing treatment, but the surface layer was still maintained as SrO after the annealing.

We investigated a systematic development of core-level spectra of Si $2p$ core levels measured on the SrO/Si specimens as a function of the duration of the post-annealing treatment at 600∘C. The intensity of the silicate peak increases with increasing annealing time. The increase was seen remarkable in the first 20 minutes, then become slow-

ly. Consequently, interfacial SiO_2 formations were not observed. This indicates that the interfacial silicate layer grew up at the initial stage of the post-annealing treatment, and the Sr-silicate inhibited the formation of SiO_2 layers. Analysis of the intensity ratios of the overlayer peaks to the substrate peaks evaluated the overlayer thicknesses. [9] Figure 2 shows thickness of overlayer silicate (or silica for the reference) as a function of the annealing time. The thickness of the interfacial silicate layer for the as-deposition sample was about 0.3 nm, and the resulting thickness after the post annealing for 120 min was 12 nm. This value corresponds to that almost overlyaer SrO becomes Sr-silicate by the annealing.
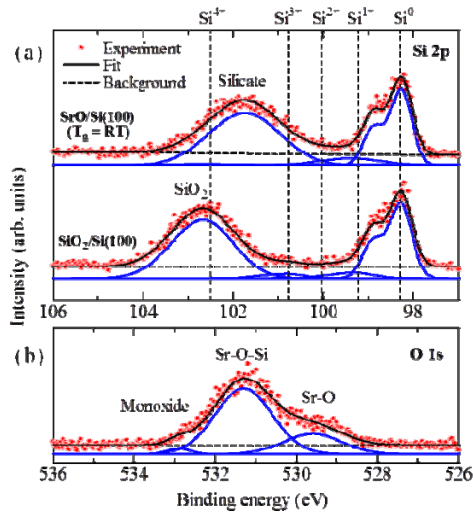

Fig. 1 (a) Si 2p and (b) O 1s core-level spectra for the SrO/Si(100) sample annealed at 600℃ for 120 min.
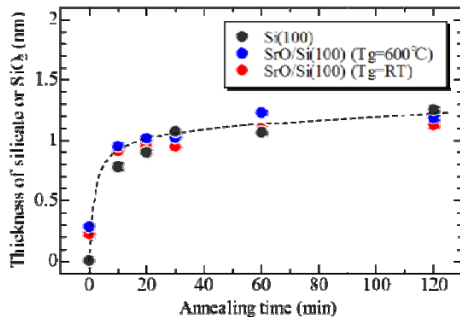

Fig. 2 The time development of the interfacial silicate thickness on the SrO/Si(100) specimens as a function of the annealing time, together with that for the reference Si(100) shown in the black dots (●). The annealing temperature was 600℃.

Finally, we deal an anomalous behavior of XPS spectra for the annealed samples. We plotted Sr 3d and the Si 2p core-level spectra using the relative binding energy in Fig 3. Here, the peak distance between Sr 3d and Si 2p (BE_{Sr3d} - BE_{Si2p}) decreases with increasing annealing time. On the other hand, the peak shape for Sr 3d and thickness of Sr-silicate (see Fig. 2) were almost constant through the annealing treatments. We infer from these results that the

Sr-silicate layer induces some positive fixed charge (or dipole) at the interface. This prediction accounts for the energy shift and inspires us the modulation of energy band discontinuity at the Sr-silicate/Si interface. Further research using electrical measurements is required to access the interfacial electronic structure.
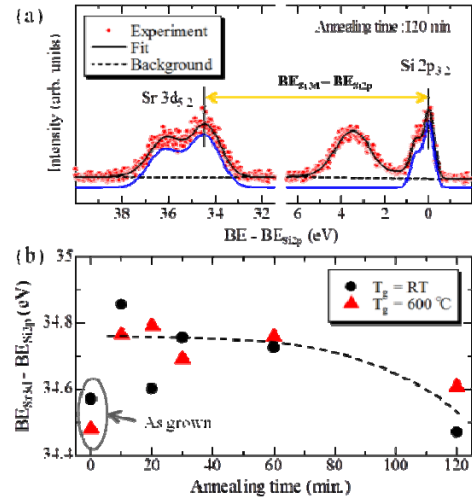

Fig. 3 (a) Sr 3d and Si 2p core-level spectra for the SrO/Si(100) samples annealed for 120 min. The binding energy is normalized with reference to Si 2p position. (b) Peak distance between energy positions of Sr 3d and Si 2p as a function of the annealing time. The data for the as-grown samples is ignored in this series.

4. Conclusions

We fabricated the SrO/Si(100) structures by PLD and investigated effect of oxygen annealing on the structure. All of the SrO reacted with the interface Si and became Sr-silicate. After the fully reaction of the SrO layer, the structure inhibited the interfacial oxidization of Si and there was absent of SiO_2 layers. Anomalous decrease of energy distance between the Sr 3d and the Si 2p core-level peaks is observed. In order to explain this decrease, we suppose that some positive charge appeared at the interface. If the charge induction really does happen, it would be favorable to device applications.

References
[1] W.F. Xiang et al, J. Cryst. Growth 271 (2004) 165, J. Wang et al, Appl. Phys. Lett. 85 (2004) 2574, C. Rossel et al, Appl. Phys. Lett. 89 (2006) 053506.
[2] J.-P. Locquet et al, J. Appl. Phys. 100 (2006) 051610.
[3] J. F. Scott, *Ferroelectric Memories, Springer, Berlin*, (2000).
[4] S. Jin et al, J. Appl. Phys, 76 (1994) 6929.
[5] M. K. Wu et al, Phys. Rev. Lett. 58 (1987) 908.
[6] R. A. Mckee et al, Phys. Rev. Lett. 81 (1998) 3014.
[7] Y. Wei et al, J. Vac. Sci. Technol. B 20 (2002) 1402.
[8] T. Yasuda et al, J. Vac. Sci. Technol. A 11, (1993) 945.
[9] F. J. Himpsel et al., Phys. Rev. B 38, 6084 (1988)
[10] J. H. Oh et al., Phys. Rev. B 63, 205310 (2001)
[11] J. Zachariae and H. Pfnür, Phys. Rev. B 72 (2005) 075410.
[12] Y. Liang et al., Appl. Phys. Lett. 79 (2001) 3591.